Injectable Silk Protein Microparticle-based Fillers: A Novel Material for Potential Use in Glottic Insufficiency

*,[1]Joseph E. Brown, *,[1]Christopher P. Gulka, *Jodie E.M. Giordano, *Maria P. Montero, *Anh Hoang, and †Thomas L. Carroll, *Medford, and †Boston, Massachusetts

Summary: Objectives and Hypothesis. A novel, silk protein-based injectable filler was engineered with the intention of vocal fold augmentation as its eventual intended use. This injectable filler leverages the unique properties of silk protein's superior biocompatibility, mechanical tunability, and slow *in vivo* degradation to one day better serve the needs of otolaryngologists. This paper intends to demonstrate the mechanical properties of the proposed novel injectable and to evaluate its longevity in animal models.

Materials and Methods. Experimental. The mechanical properties of silk bulking agents were determined to characterize deformation resistance and recovery compared with commercially available calcium hydroxylapatite through rheologic testing. Fresh porcine vocal fold tissue was used for injectable placement to simulate the mechanical outcomes of native tissue after bulking procedures. *In vivo* subcutaneous rodent implantation examined immune response, particle migration, and volume retention.

Results. Porous, elastomeric silk microparticles demonstrate high recovery (>90% original volume) from compressive strain and mimic the native storage modulus of soft tissues (1−3 kPa). Injectable silk causes only a slight increase in porcine vocal fold stiffness immediately after injection (20%), preserving the native mechanics of bulked tissue. In the subcutaneous rat model, silk demonstrated biocompatibility and slow degradation, thus enabling host cell integration and tissue deposition.

Conclusions. The presented novel silk injectable material demonstrates favorable qualities for a vocal fold injection augmentation material. An *in vivo* long-term canine study is planned.

Key Words: Silk−Vocal fold−Vocal fold injectable−Microparticle−Injection augmentation.

INTRODUCTION

Glottic insufficiency (GI) exists when the normally symmetric true vocal folds (TVFs) cannot meet and achieve a long, complete phase closure during vibration. Injection augmentation and medialization laryngoplasty both bulk the vocal fold tissue to enable the vocal folds to contact each other and restore efficient entrainment of vibration. Injection augmentation is increasingly popular, likely because of the availability of off-the-shelf injectable materials and the ability to perform these procedures as an awake, unsedated office-based procedure.[1] A variety of material choices are available for injection augmentation, including autologous fat, hyaluronic acid (HA), collagen, carboxymethylcellulose (CMC), and calcium hydroxylapatite (CaHA)-based fillers. Medialization laryngoplasty is a permanent option to correct GI but requires an incision in the neck and sedation in the operating room to implant a permanent material such as Gore-Tex or silastic in the deficient vocal fold.[2,3] An unmet medical need is an office-based, injectable material that can sustain medialization by enabling tissue regrowth within the bulked vocal fold leading to a long-term or even permanent effect.

Silk, as derived from the *Bombyx mori* silk worm, has an extensive history as a surgical biomaterial.[4] Silk has been used for centuries as a suture material and continues to remain a popular choice for neural, ocular, and cardiovascular applications because of its inherent high tensile strength and favorable handleability.[5−7] Commercially available silk-derived surgical scaffolds are currently used for long-term soft tissue regeneration and reconstructive surgery.[8−12] Results indicate that controlled degradation of porous silk scaffolds implanted into soft tissues facilitates cellular infiltration and encourages tissue regeneration and remodeling within the implant site, giving rise to the potential of a permanent tissue bulking treatment.[10,12,13]

In the current study, the goal was to develop a robust, injectable silk particle suspension for potential use in GI. Particle suspensions were designed for high porosity, low immunogenic response, mechanical similarity to native tissues, facile injection, and long-term *in vivo* persistence. Safety and tissue response to implants was investigated using a subcutaneous rat model. We hypothesized that (1) biocompatible silk particles would bulk fresh, cadaver porcine vocal fold tissues without causing excessive stiffening of tissues, and (2) while simultaneously providing a scaffold for cellular ingrowth and tissue deposition in a subcutaneous rat model, long-lasting modification due to the inherent slow resorption rate of silk proteins would be seen.

MATERIALS AND METHODS

Materials

Sodium carbonate, lithium bromide, sodium hydroxide, hydrochloric acid, 1,4-butanediol diglycidyl ether, and glycerol were

Accepted for publication January 18, 2018.
This work was performed at Sofregen Inc., 200 Boston Avenue, Medford MA, 02155.
Financial disclosure: Thomas Carroll discloses consulting fees from Sofregen Inc.
From the *Sofregen, Inc., Medford Massachusetts; and the †Brigham and Women's Hospital, Department of Otolaryngology, Boston, Massachusetts.
[1]These authors contributed equally to this study.
Address correspondence and reprint requests to Thomas L. Carroll, Department of Otolaryngology, Brigham and Women's Hospital, 45 Francis St. Boston, MA 02115. E-mail: tcarroll@BWH.Harvard.edu
Journal of Voice, Vol. 33, No. 5, pp. 773−780
0892-1997

https://doi.org/10.1016/j.jvoice.2018.01.017

purchased from Millipore Sigma (St. Lewis, MS). Methanol was purchased from VWR International (Radnor, PA). Sodium hyaluronate was purchased from Lifecore Biomedical (Chaska, MN). All chemicals and materials were used without further modification unless specified.

Preparation of porous silk protein microparticles

Raw medical-grade silk fiber was purified as previously described.[13] Briefly, the raw silk fibers were extracted for 60 minutes in a 2.12 g/L sodium carbonate solution to remove sericin coating. Silk fibers were solubilized and subsequently dialyzed against deionized water to yield a 10% w/v solution. Silk solutions were freeze-dried in the presence of glycerol, cross-linked with methanol, and mechanically ground into 355- to 425-μm particles.

Preparation of HA carrier and particle suspension

HA (1.50 g) was first hydrated in sodium hydroxide (10.725 mL, 0.25 M) for 2 hours. Afterward, 72.8 mM 1,4-butanediol diglycidyl ether was added into the HA suspension and allowed to cross-link for 2 hours between 45°C and 50°C. Cross-linked gel was quenched with 30 mL 1× phosphate-buffered saline overnight. Hydrogels were then dialyzed against phosphate-buffered saline to a final concentration of 2.7% w/v and a pH of 7.4. Silk particles and cross-linked HA (hereafter "silk-HA") were steam sterilized and aseptically mixed in a 40% silk/60% HA v/v ratio.

Characterization of porous silk scaffolds

Scanning electron microscopy (Zeiss EVO MA10 SEM; Carl Zeiss AG, Germany) was used to analyze the morphology of bulk sponge cross sections and porous microparticles. Porosity and pore size distribution of bulk sponges were tested with a Quantachrome PoreMaster mercury intrusion porosimeter (Quantachrome Instruments, Boynton Beach, FL). Unconfined compression testing on hydrated samples was performed on an Instron 3366 Universal Testing System (Instron, Norwood, MA) and used to evaluate compressibility and recovery of silk sponge samples (measurements reported in kilopascal). Microparticle size distribution was measured using a Mastersizer 2000 laser diffraction tool (Malvern Instruments, Worcestershire, UK).

Injection force testing through catheter

Uniaxial compression testing was used to determine the extrusion force required for injection of silk-HA through a catheter delivery device and CaHA-CMC through the included 24G long needle. A custom 50-cm catheter (inner diameter: 1.05 mm) affixed with a 23XXG needle (inner diameter: 0.508 mm) was designed to accommodate delivery of silk-HA through the working channel of a laryngoscope. One-cubic centimeter threaded nozzle plastic syringes prefilled with silk-HA composition were loaded into a vertical syringe mount and extruded using an Instron 3366 mechanical testing system (Instron) with an attached 1 kN load cell. Compressive force was applied to the top of the plunger at a constant rate of 13 mm/min. Average extrusion force (reported in newton) was measured during the plateau phase (between 70% and 100% extruded volume for silk-HA, and between 15% and 100% extruded volume for CaHA-CMC).

Dynamic rotational shear rheometry

Dynamic rotational shear rheometry was used to assess the mechanical features of silk-HA compositions and bulked porcine vocal fold tissue.[14,15] The storage modulus (G', reported in pascal), the loss modulus (G'', reported in pascal), the complex modulus (G^*, reported in pascal), and dynamic viscosity (reported in pascal-second) were measured as a function of oscillatory frequency sweeps from 0.1 to 10.0 Hz at a shear strain of 1%. Testing was performed on a Discovery HR-3 (TA Instruments, New Castle, DE) using a 40-mm-diameter parallel plate attachment. For silk-HA compositions, the nominal gap width used was 400 μm to accommodate the size of the particles with a sample volume of 500 μL. Elasticity was calculated from Equation 1 at frequencies of 1 and 10 Hz:

$$\text{Elasticity} = 100 \times [G'/(G' + G'')] \quad (1)$$

In vitro tissue bulking of porcine vocal fold tissue

Fresh porcine larynges were bisected through the anterior commissure to expose the intact vocal folds, and 250−300 μL of silk-HA composition was directly injected deep into the thyroarytenoid-lateral cricoarytenoid muscle complex to avoid superficial injection into the lamina propria (Supplementary Figure S1). Vocal folds were excised (including the thyroarytenoid muscle), cut to approximately 1 cm × 1 cm dimensions, and the mechanics of noninjected ("native") and injected ("bulked") tissues were assessed by dynamic rotational shear rheometry using the system described previously. Four hundred-grit sandpaper was used to reduce slippage. The gap distance was modulated to achieve an axial force of 40−50 g.

In vivo biodegradation of silk-HA formulation

Animal procedures were carried out in full accordance with established standards set forth in the Guide for the Care and Use of Laboratory Animals, 8th edition (NIH Publication No. 85-23). Animals were sterilely housed and maintained pre- and postoperatively by the Department of Lab Animal Management and associated veterinarians at the Tufts University, Boston Campus. Two separate studies were conducted to evaluate (1) the biocompatibility of the silk-HA formulation compared with a marketed CaHA-CMC filler (Prolaryn Plus; Merz Neurosciences, Raleigh, NC) and (2) the degradation profile of silk particles. A subcutaneous model using rats (female, 8 weeks; Taconic Biosciences, Germantown, NY) was used in both studies. Rats were anesthetized by isoflurane inhalation, 3% for inoculation, and 2% for maintenance. For evaluation of biocompatibility, N = 3 animals per time point received subcutaneous injections of 0.2 mL silk-HA or CaHA-CMC to each of the left and right sides in the lumbar region. Time points of 3, 6, 9, and 12 months were selected to assess the progressive host ingrowth and immunologic response of the injections.

In vivo biodegradation of silk particles

For evaluation of silk particle degradation, animals received four subcutaneous injections of 0.2 mL silk particles alone on the left and right sides of the lumbar and scapular regions. A total of 15 animals received injections, with N = 3 for time points of 1, 3, 5, 9, and 12 months. Animals were sacrificed by carbon dioxide asphyxiation and major organ removal as a secondary method. Samples were excised, including the adjacent dermal tissue, and dimensions (length, width, and height) of the remaining implant were recorded. Explants were placed into tissue cassettes and immersed in 10% formalin for fixation. Tissues were taken through standard dehydration processing and bisected before paraffin embedding. Tissue sections were stained using hematoxylin and eosin and imaged using an inverted light microscope (Axiovert CFL 40, Carl Zeiss AG, Switzerland) and *Q-Capture* software (QImaging, Surrey, BC).

Data reporting and statistics

Pore and particle size distributions are reported as the average of three unique material batches. Rheometry results for silk-HA suspensions were reported as the average with standard deviation for N = 3.

RESULTS

Characterization of porous silk microparticles and catheter injection force testing

The physical characteristics of the silk particles, including porosity, shape memory characteristics, and size distribution, are shown in Figure 1. Bulk sponges are composed of a highly interconnected pore network, with rounded pore diameters averaging between 10 and 100 μm (Figure 1A and B). These bulk sponges also display shape memory features, having the ability to recover their original volume from a compressed state (Figure 1C). Cyclic compression curves of sponges immersed in physiological buffer show high recovery and minimal hysteresis under low to moderate strains, highlighting their resistance to deformation (Figure 1D). Deformation resistance and recovery are critical for recapitulating the elastomeric behavior of native vocal fold tissue, allowing the implant to feel and perform similarly to healthy tissue. Particles derived from bulk sponges possess the same open-pore morphology, presenting the appearance of large microparticle sponges (Figure 1E and F). Open-pore morphology may accommodate applications where cell infiltration and tissue regeneration are required.[16,17]

The injection force of silk-HA was measured when delivered through a custom 50-cm catheter (Figure 2). The custom catheter is designed to fit through the working channel of popular laryngoscopes and disposable channel sheaths, enabling the physician to visualize the delivery of the material during an augmentation procedure (Figure 2A and Supplementary Figure S2). The catheter includes a retractable 23XXG needle to enable controlled and reproducible delivery of material (Figure 2B and C). At 13-mm/min crosshead speed, the average extrusion force of silk-HA through the catheter was 34.9 N $\pm$ 1.6 N, whereas CaHA-CMC extruded through a 24G long needle was 51.4 N $\pm$ 0.9 N (Figure 2D).

Mechanical analysis of *ex vivo* bulked vocal fold tissue

Oscillatory shear deformation was used to measure the shear moduli (G' and G'', the overall resistance to deformation), dynamic viscosity (flow characteristics), and elasticity (deformation recovery) of injectable materials as a function of frequency. The mechanical attributes of the silk injectable were compared with CaHA-CMC, a commercially available particle-based vocal fold filler (Supplementary Figure S3). Oscillatory frequency sweeps from 0.1 to 10.0 Hz demonstrate that both silk and CaHA-CMC behave elastically over the tested range. The stiffness of CaHA-CMC increases more rapidly than silk, with a nearly fivefold increase in storage modulus over the frequency range tested and silk showed superior deformation recovery.

The mechanical impact of silk and CaHA-CMC bulking was evaluated by injection into porcine vocal fold tissues on the bench, to be used as an approximation for what clinical outcomes may be after a vocal fold bulking procedure. Similar *ex vivo* mechanical screening for vocal fold bulking agents has been described previously in the literature.[15,18] Excised larynx samples from two different age groups of pigs (2 and 7 weeks old) were injected *ex vivo* via a 21G (silk injectable) or a 25G (CaHA-CMC) needle affixed to a 1-cc syringe. Native and bulked vocal folds were excised and mechanics were evaluated via shear rheometry (Figure 3). It was noted that, because the excised tissue samples did not contact the entirety of the parallel plates during testing, absolute values were uncertain, and that the data served to highlight comparable trends rather than true values. After bulking, silk yielded minimal change in tissue viscoelasticity, increasing the complex modulus by approximately 1.5× and 1.2×, whereas CaHA-CMC bulking increased modulus by approximately 4.0× and 1.7× in 2- and 7-week-old pigs, respectively (Figure 3A and B). Dynamic viscosity reflected similar trends, with CaHA-CMC incurring the greatest increase in tissue stiffness (Figure 3C). Deformation recovery for injected tissues was only slightly altered compared with native tissues for both materials (Figure 3D).

In vivo evaluation of silk particle suspensions

In a 12-month study of biocompatibility, silk-HA and CaHA-CMC exhibited similar cellular responses of macrophage and fibrous tissue infiltration around implanted particles (Figure 4). Post implantation, both particle suspensions did not migrate from the delivery site after the 12-month period. In hematoxylin- and eosin-stained sections, macrophages and giant cells predominated in the vicinity of silk particles within 3 months (Supplementary Figure S4), with few multinucleated cells visible, and appeared to be actively degrading the protein matrix. Macrophage activity typically recruits fibroblasts to the site of remodeling, leading to interstitial fibrous tissue deposits, which are also observed in silk implants. It was additionally noted that cross-linked HA carrier controls (without silk component) were void of cellular infiltrate, indicating that silk particles were critical to cell ingrowth and remodeling (Supplementary Figure S4). The CaHA-CMC implants permitted cell migration around the particles but did not allow infiltration into the particle bulk as seen with silk.

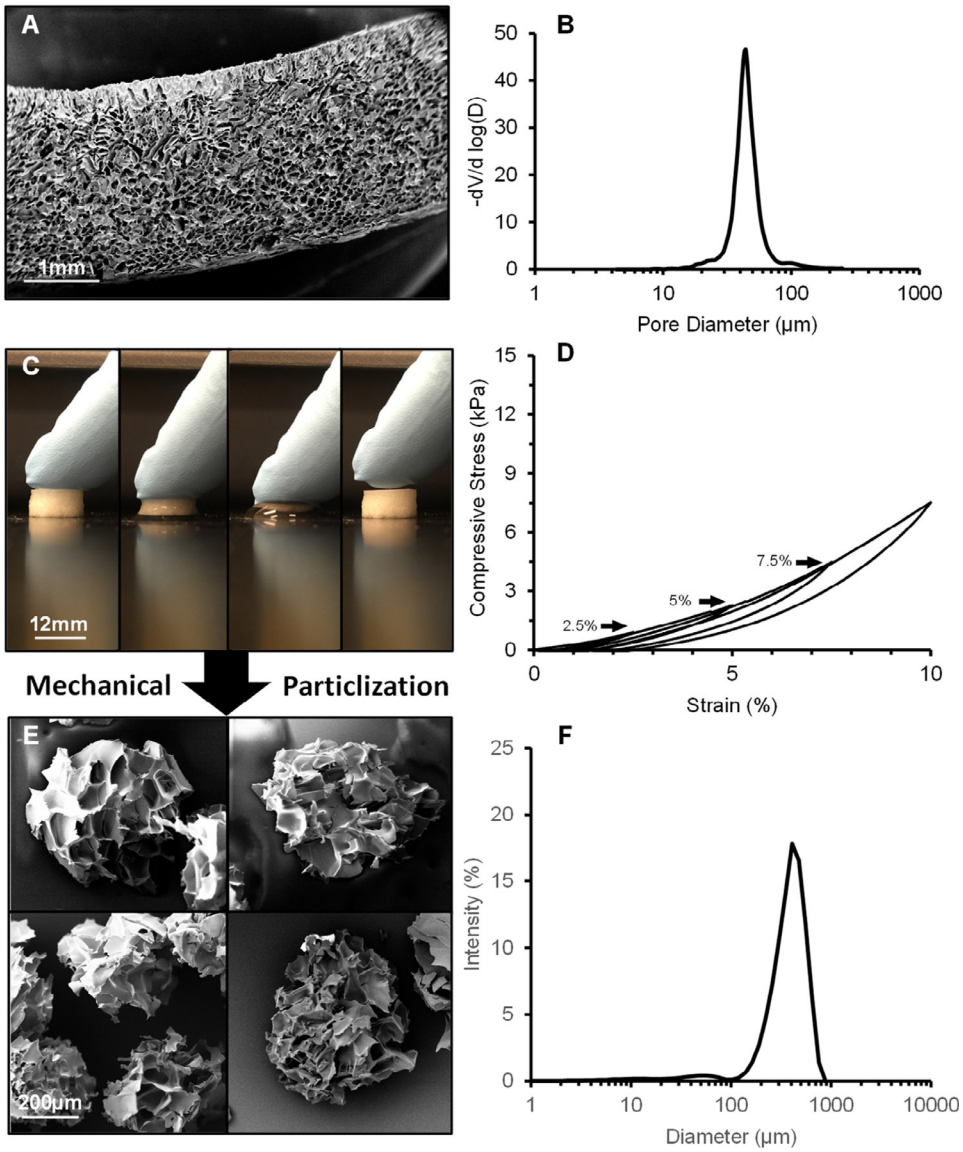

FIGURE 1. Physical characterization of porous silk sponges and particles. **A.** Scanning electron microscopy showing a cross section of the bulk silk sponge and the inner pore morphology. **B.** The average pore size, as determined by mercury intrusion porosimetry, is 40 μm. **C.** Macroscopic depiction of shape memory potential for silk sponges. A hydrated silk sponge can recover from a highly compressed state to nearly its original volume. **D.** Cyclic compression curves showing high recovery of the sponge when immersed in 1× phosphate-buffered saline. **E.** Porous silk microparticles are derived from the bulk via a mechanical particlization method. **F.** The average particle diameter is measured at 390 μm via laser diffraction.

The goal of these early biocompatibility assessments was to evaluate particle degradation kinetics and inflammatory response with regard to severity of inflammation around the implant. Macroscopic evaluation of animal livers was performed *in situ* at sacrifice for any lesions or signs of material migration. All livers were a standard dark red and appeared to be of normal tissue health and weight. The silk particle suspension is highly cohesive, and we observed very minimal local migration of the bulk material away from the initial injection site. Because we did not see an extreme response, pathologist evaluation was not pursued; no signs of infection or other unexpected findings warranted seeking an expert opinion at this proof-of-concept stage.

In vivo biodegradation of silk particles

A separate biocompatibility study was initiated to better assess the degradation profile and the longevity of silk particles alone without a carrier matrix. Silk particle implants degraded linearly over the course of the study; and extrapolation of this linear trend projects the silk particles remaining present until nearly 18 months from implantation, at which time complete degradation is predicted to occur (Supplementary Figure S5).

DISCUSSION

The ideal TVF injection augmentation material needs to be biocompatible, available off the shelf, nonimmunogenic,

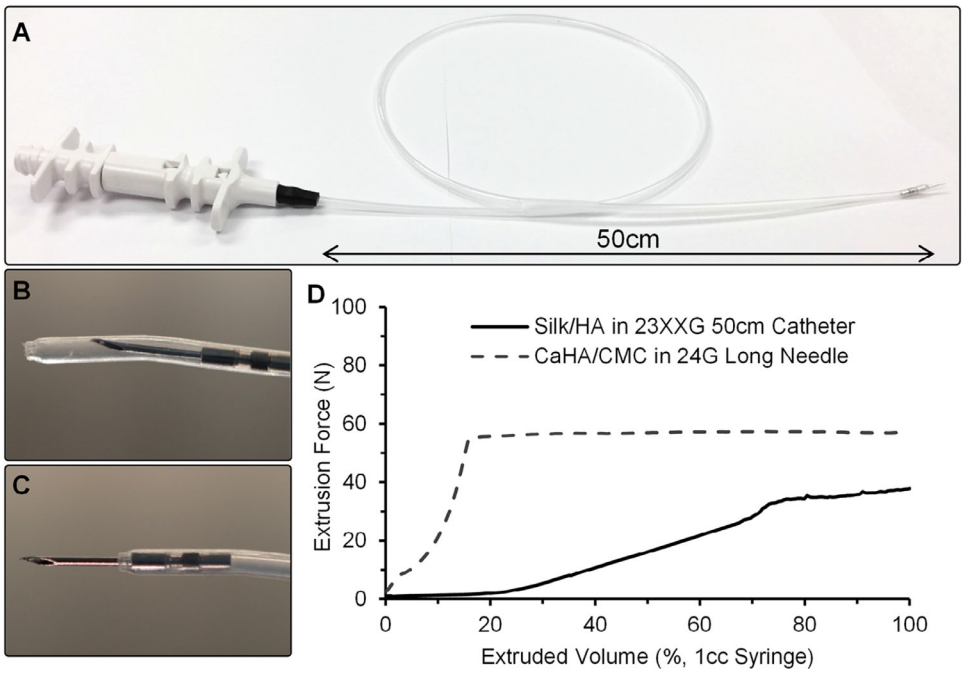

FIGURE 2. Injection force analysis of silk-HA and CaHA-CMC. **A–C.** Silk-HA was extruded through a 50-cm custom catheter, designed with a retractable 23XXG needle. CaHA-CMC was extruded through a 24G long needle (not shown). **D.** Injection forces were measured at a crosshead speed of 13 mm/min. The average injection force of silk-HA was 34.9 N ± 1.6 N, whereas CaHA-CMC extruded through a 24G long needle was 51.4 N ± 0.9 N. Typically, lower extrusion forces are ideal because they reduce discomfort for the user.

without concern for disease transmission, able to flow through a small gauge needle, and easy to use and facilitates long-lasting results when desired. The presented silk-HA injectable shows promise as a potential TVF injection augmentation material to meet these criteria. The cross-linking density, HA concentration, and silk : HA ratio selected yielded an optimal balance between low extrusion force, ideal rheometric features, and *in vivo* longevity. Although not yet tested *in vivo* and in muscle, the current study does demonstrate promise in that silk particles have potential for a long-term, durable benefit with the addition of improved rheologic properties over currently available CaHA injectables after immediate injection.

Particle morphology and rheometric analysis

Silk particles were engineered to have a defined open-pore, low-density, elastomeric structure to best facilitate the ingrowth of cells and replicate the native tissue features. This is unique compared with other commercially available filler platforms that utilize solid particles or hydrogel particles that rely on surface erosion to degrade. Although porous silk particles are large (average diameter: 390 μm), the inherent shape memory features permit the reversible compressibility needed for particles to flow through narrow channels without compromising their porous structure. Furthermore, several studies have indicated that particles less than 65 μm may be at risk of migration to regional lymphatic pathways.[19–22] Therefore, silk particles were engineered to be larger to greatly mitigate risk of migration into the vasculature. Combined with the inherently slow biodegradation rate of silk,[23,24] we anticipate that gradual replacement of the bulk silk matrix over time may facilitate tissue regeneration and vascularization at early time points, as reported previously for large porous silk implants.[10,12]

The mechanical behavior of silk particle suspensions makes it ideal for vocal fold applications, where frequency independence and low stiffness are beneficial in replicating the native tissue properties.[15] CaHA was chosen as a comparator in these studies as it is widely used in the field for vocal fold augmentation and is the only comparable product with Food and Drug Administration clearance for vocal fold medialization, providing a well-known product as a reference for comparison with the novel silk particle-based filler. Two age groups for porcine vocal fold were tested, because aging is known to increase collagen density and tissue stiffening.[25] As expected, tissues from younger animals showed greater susceptibility to stiffening after injection; however, compared with CaHA-CMC particle suspensions, bulking with silk induces substantially less stiffening in both age groups. This difference may be attributed to the enhanced elasticity of the silk compositions, as well as the inherent shape recovery attributes of the silk particles. Our results are in alignment with previously published *ex vivo* injection laryngoplasty experiments where CaHA-CMC bulking caused the augmented vocal fold tissue to become stiffer, whereas hyaluronic-based materials were able to better mimic the native tissue mechanics.[15,26–29] Although time and tissue integration would likely change the measurements from what the present study's immediate postinjection tissues demonstrate in fresh porcine larynges, these results encourage

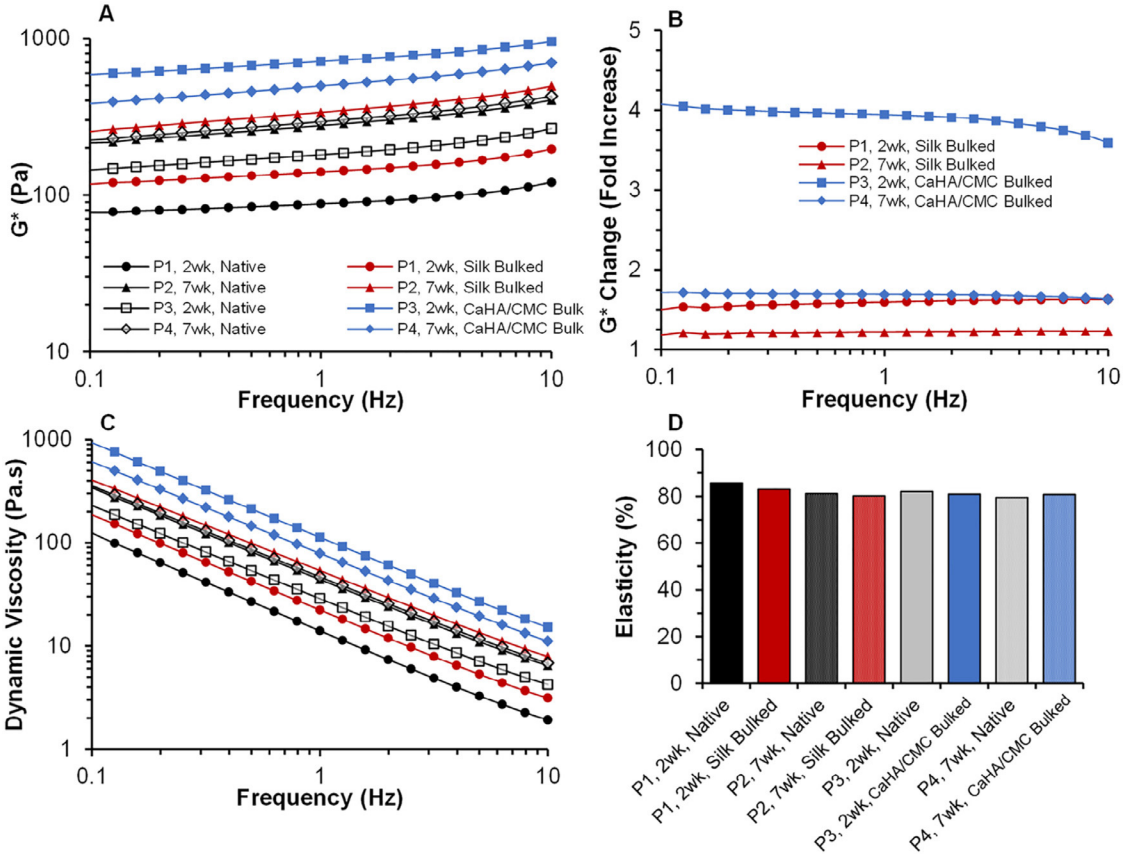

FIGURE 3. Rotational shear rheometry measurements of porcine vocal fold tissue from 2- and 7-week-old pigs after bulking with silk-HA and Prolaryn Plus. **A.** Frequency sweeps measuring complex modulus showed that silk-HA bulking incurred little change to the native tissue mechanics. **B.** The fold change of bulked tissue was at most 1.5× for silk-HA and up to 4× for Prolaryn Plus. **C.** Dynamic viscosity measurements indicate that Prolaryn Plus induces the greatest increase in tissue stiffness. **D.** Elasticity of all tissues was similar, and bulking did not greatly impact deformation recovery.

the further exploration of *in vivo* canine thyroarytenoid muscle placement.

In vivo biocompatibility

The silk-HA suspension is designed not only to volumetrically bulk damaged tissue but also to provide long-lasting augmentation via a dynamic, resorbable scaffold that can support cell attachment and new collagen formation simultaneous to gradual silk degradation. This approach has been validated using CaHA-CMC microparticle suspensions for vocal fold augmentation. A clinical study of CaHA-CMC fillers has shown that stimulation of new tissue formation within the implant can prolong duration of correction and patient satisfaction.[30–32] The results indicate many patients benefitting from voice improvement 12–18 months post treatment.[31,33]

Silk proteins provide an alternative platform recognized for controllable long-term resorbability, biocompatibility, and regenerative capacity of new tissues at an implant site.[34] Our prediction for a longer-term effect stems from the results of our study in conjunction with previously published silk surgical scaffold studies examining tissue ingrowth and bioreplacement of implantable silk.[8,10,11] Uniformly porous silk meshes have demonstrated the ability to support and repair soft tissues while facilitating postsurgical tissue remodeling and neovascularization for long-term regeneration.[11,12] We sought to leverage these benefits, such as the early recruitment of localized collagen deposition, angiogenic factors, and cellular infiltration, into a new porous microparticle platform ideal for minimally invasive delivery. The 12-month results of injectable silk-HA reported in the current study affirm that within 3–6 months, macrophage ingrowth—a typical precursor to fibroblast recruitment and interstitial fibrous tissue deposition[35]—and silk protein degradation occur without eliciting any adverse reaction in a subcutaneous rat model. The outcome of the present pilot study is encouraging and prompts the continued investigation of silk particle efficacy in a 12-month *in vivo* canine vocal fold augmentation model.

CONCLUSIONS

The objective of the present pilot study was to evaluate the mechanical performance, safety, and biological response of an injectable silk particle suspension that is being designed specifically with the intention of serving as a novel vocal fold augmentation material. Silk-HA is a porous, silk microparticle

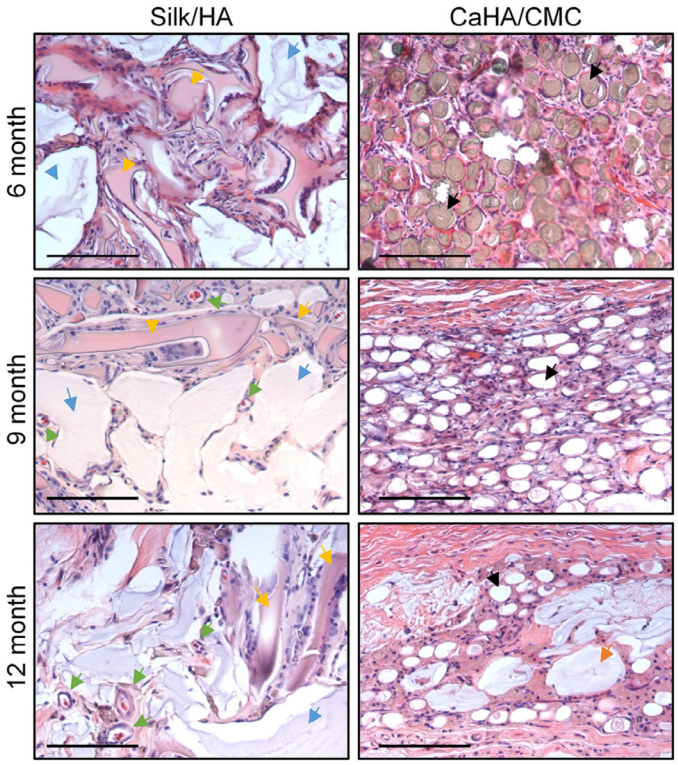

FIGURE 4. *In vivo* biocompatibility study of porous silk particles using a subcutaneous rat model, 20× magnification. Histologic examination of excised implants was performed on silk-HA (*left column*) and CaHA-CMC (*right column*) at 6, 9, and 12 months, descending. Cellular infiltration is observed in the vicinity of the silk particles (*yellow arrows*) and is predominantly macrophages and giant cells responsible for enzymatic degradation of the silk protein. Silk-HA cross sections show vascularity (*green arrows*) within the tissue ingrowth. Regions of HA (*blue arrows*) are cell occlusive and collapse with histologic processing. CaHA-CMC also supports macrophage and giant cell infiltration in the vicinity of the CaHA particles (*black arrows*). Both 9- and 12-month sections were decalcified before staining, resulting in ghost regions where the CaHA particles were previously. Similar to HA, CMC (*orange arrow*) is cell occlusive. Vascularity is not visible in the CaHA-CMC tissue sections represented *above* in the right hand column (Scale bar = 0.125 mm). (For interpretation of the references to color in this figure legend, the reader is referred to the Web version of this article.)

suspension that demonstrates highly elastic mechanics that have been modulated and mimic the native rheometric features of porcine vocal fold, volumetrically bulking the tissue without causing excessive stiffening. Silk-HA suspensions were evaluated in a 6-month subcutaneous rat model against CaHA-CMC. Silk particle implants showed macrophage infiltration and fibrous tissue deposition throughout the particle bulk without eliciting any adverse reactions, including swelling or migration from the primary site. Silk-HA shows promise as a potential injectable material for vocal fold augmentation and will continue to be investigated in longer preclinical *in vivo* vocal fold implantation studies.

Acknowledgment

The authors thank DaVinci Biomedical for its generous donation of porcine vocal fold tissue.

SUPPLEMENTARY DATA

Supplementary data related to this article can be found online at doi:10.1016/j.jvoice.2018.01.017.

REFERENCES

1. Mallur PS, Rosen CA. Vocal fold injection: review of indications, techniques, and materials for augmentation. *Clin Exp Otorhinolaryngol*. 2010;3:177–182. https://doi.org/10.3342/ceo.2010.3.4.177.
2. Rudolf R, Sibylle B. Laryngoplasty with hyaluronic acid in patients with unilateral vocal fold paralysis. *J Voice*. 2012;26:785–791. https://doi.org/10.1016/j.jvoice.2011.11.007.
3. Vachha BA, Ginat DT, Mallur P, et al. "Finding a voice": imaging features after phonosurgical procedures for vocal fold paralysis. *AJNR Am J Neuroradiol*. 2016;37:1574–1580. https://doi.org/10.3174/ajnr.A4781.
4. Omenetto FG, Kaplan DL. New opportunities for an ancient material. *Science*. 2010;329:528–531. https://doi.org/10.1126/science.1188936.
5. Salthouse T, Matlaga B, Wykoff M. Comparative tissue response to six suture materials in rabbit cornea, sclera, and ocular muscle. *Am J Ophthalmol*. 1977;84:224–233.
6. Rossitch E, Bullard DE, Oakes WJ. Delayed foreign-body reaction to silk sutures in pediatric neurosurgical patients. *Childs Nerv Syst*. 1987;3:375–378. https://doi.org/10.1007/BF00270712.
7. Altman GH, Diaz F, Jakuba C, et al. Silk-based biomaterials. *Biomaterials*. 2003;24:401–416.
8. Bellas E, Rollins A, Moreau JE, et al. Equine model for soft-tissue regeneration. *J Biomed Mater Res B Appl Biomater*. 2015;103:1217–1227. https://doi.org/10.1002/jbm.b.33299.
9. Etienne O, Schneider A, Kluge JA, et al. Soft tissue augmentation using silk gels: an in vitro and in vivo study. *J Periodontol*. 2009;80:1852–1858. https://doi.org/10.1902/jop.2009.090231.
10. Bellas E, Panilaitis BJB, Glettig DL, et al. Sustained volume retention in vivo with adipocyte and lipoaspirate seeded silk scaffolds. *Biomaterials*. 2013;34:2960–2968. https://doi.org/10.1016/j.biomaterials.2013.01.058.
11. Gross JE, Horan RL, Gaylord M, et al. An evaluation of SERI surgical scaffold for soft-tissue support and repair in an ovine model of two-stage breast reconstruction. *Plast Reconstr Surg*. 2014;134:700e–704e. https://doi.org/10.1097/PRS.0000000000000697.
12. Kijanska M, Marmaras A, Hegglin A, et al. In vivo characterization of the integration and vascularization of a silk-derived surgical scaffold. *J Plast Reconstr Aesthet Surg*. 2016;69:1141–1150. https://doi.org/10.1016/j.bjps.2016.01.017.
13. Rockwood DN, Preda RC, Yücel T, et al. Materials fabrication from *Bombyx mori* silk fibroin. *Nat Protoc*. 2011;6:1612–1631. https://doi.org/10.1038/nprot.2011.379.
14. Miri AK. Mechanical characterization of vocal fold tissue: a review study. *J Voice*. 2014;28:657–667. https://doi.org/10.1016/j.jvoice.2014.03.001.
15. Caton T, Thibeault SL, Klemuk S, et al. Viscoelasticity of hyaluronan and nonhyaluronan based vocal fold injectables: implications for mucosal versus muscle use. *Laryngoscope*. 2007;117:516–521. https://doi.org/10.1097/MLG.0b013e31802e9291.
16. Rnjak-Kovacina J, Wray LS, Burke KA, et al. Lyophilized silk sponges: a versatile biomaterial platform for soft tissue engineering. *ACS Biomater Sci Eng*. 2015;1:260–270. https://doi.org/10.1021/ab500149p.
17. Lutolf MP, Hubbell JA. Synthetic biomaterials as instructive extracellular microenvironments for morphogenesis in tissue engineering. *Nat Biotechnol*. 2005;23:47–55. https://doi.org/10.1038/nbt1055.
18. Hertegard S, Dahlqvist A, Laurent C, et al. Viscoelastic properties of rabbit vocal folds after augmentation. *Otolaryngol Head Neck Surg*. 2003;128:401–406. https://doi.org/10.1067/mhn.2003.96.

19. Henly DR, Barrett DM, Weiland TL, et al. Particulate silicone for use in periurethral injections: local tissue effects and search for migration. *J Urol*. 1995;153:2039–2043.
20. Beisang AA, Ersek RA. Mammalian response to subdermal implantation of textured microimplants. *Aesthetic Plast Surg*. 1992;16:83–90.
21. Allen O. Response to subdermal implantation of textured microimplants in humans. *Aesthetic Plast Surg*. 1992;16:227–230.
22. Sittel C, Thumfart WF, Pototschnig C, et al. Textured polydimethylsiloxane elastomers in the human larynx: safety and efficiency of use. *J Biomed Mater Res*. 2000;53:646–650.
23. Vepari C, Kaplan DL. Silk as a biomaterial. *Prog Polym Sci*. 2007;32:991–1007. https://doi.org/10.1016/j.progpolymsci.2007.05.013. Silk.
24. Kundu B, Rajkhowa R, Kundu SC, et al. Silk fibroin biomaterials for tissue regenerations. *Adv Drug Deliv Rev*. 2013;65:457–470. https://doi.org/10.1016/j.addr.2012.09.043.
25. Hirano S, Nagai H, Tateya I, et al. Regeneration of aged vocal folds with basic fibroblast growth factor in a rat model: a preliminary report. *Ann Otol Rhinol Laryngol*. 2005;114:304–308. https://doi.org/10.1177/000348940511400409.
26. Kimura M, Mau T, Chan RW. Viscoelastic properties of phonosurgical biomaterials at phonatory frequencies. *Laryngoscope*. 2010;120:764–768. https://doi.org/10.1002/lary.20816.
27. Lisi C, Hawkshaw MJ, Sataloff RT. Viscosity of materials for laryngeal injection: a review of current knowledge and clinical implications. *J Voice*. 2013;27:119–123. https://doi.org/10.1016/j.jvoice.2012.07.011.
28. Sundaram H, Voigts B, Beer K, et al. Comparison of the rheological properties of viscosity and elasticity in two categories of soft tissue fillers: calcium hydroxylapatite and hyaluronic acid. *Dermatol Surg*. 2010;36 (s3):1859–1865. https://doi.org/10.1111/j.1524-4725.2010.01743.x.
29. Borzacchiello A, Mayol L, Ambrosio L. Rheological characterization of vocal folds after injection augmentation in a preliminary animal study. *J Bioact Compat Polym*. 2004;19:331–341. https://doi.org/10.1177/0883911504045229.
30. Caffier PP, Nasr AI, Weikert S, et al. The use of injectable calcium hydroxylapatite in the surgically pretreated larynx with glottal insufficiency. *Laryngoscope*. 2016;127:1125–1130. https://doi.org/10.1002/lary.26261.
31. Carroll TL, Rosen CA. Long-term results of calcium hydroxylapatite for vocal fold augmentation. *Laryngoscope*. 2011;121:313–319. https://doi.org/10.1002/lary.21258.
32. Marmur ES, Phelps R, Goldberg DJ. Clinical, histologic and electron microscopic findings after injection of a calcium hydroxylapatite filler. *J Cosmet Laser Ther*. 2004;6:223–226. https://doi.org/10.1080/14764170410003048.
33. Rosen CA, Gartner-Schmidt J, Casiano R, et al. Vocal fold augmentation with calcium hydroxylapatite: twelve-month report. *Laryngoscope*. 2009;119:1033–1041. https://doi.org/10.1002/lary.20126.
34. Thurber AE, Omenetto FG, Kaplan DL. In vivo bioresponses to silk proteins. *Biomaterials*. 2015;71:145–157. https://doi.org/10.1016/j.biomaterials.2015.08.039.
35. Wynn TA, Vannella KM. Macrophages in tissue repair, regeneration, and fibrosis. *Immunity*. 2016;44:450–462. https://doi.org/10.1016/j.immuni.2016.02.015.